Journal of Fluorine Chemistry 137 (2012) 64–72

Contents lists available at SciVerse ScienceDirect

Journal of Fluorine Chemistry

journal homepage: www.elsevier.com/locate/fluor

Hydrodefluorination of polyfluoro-2-naphthylamines by Zn in aqueous NH_3: A correlation of the product distribution and the computationally predicted regioselectivity of the substrate radical anion fragmentation

Galina A. Selivanova [a], Alexey V. Reshetov [a,b], Irina V. Beregovaya [a], Nadezhda V. Vasil'eva [a], Irina Yu. Bagryanskaya [a], Vitalij D. Shteingarts [a,*]

[a] N. N. Vorozhtsov Institute of Organic Chemistry, Siberian Division of the Russian Academy of Sciences, 9 Ac. Lavrentjev Avenue, Novosibirsk 630090, Russia
[b] Novosibirsk State University, Pirogova Str., 2, Novosibirsk 630090, Russia

ARTICLE INFO

Article history:
Received 13 September 2011
Received in revised form 16 February 2012
Accepted 26 February 2012
Available online 7 March 2012

Keywords:
Polyfluoro-2-naphthylamines
Hydrodefluorination
CVA measurements
Quantum-chemical calculations
X-ray analysis

ABSTRACT

Hydrodefluorination of heptafluoro-2-naphthylamine and its less fluorinated analogues by zinc in aqueous ammonia has been explored with respect to the possibility to occur and to rationalize the product distribution in terms of the mechanism including formation and fragmentation of a polyfluoroarene radical anion.

1. Introduction

Fluorine containing arylamines are valuable building blocks for synthesis of potentially bioactive fluoro compounds, particularly azaheterocycles [1]. Among fluoroanilines accessible are low fluorinated (1–2 fluorine atoms per a ring) compounds of this type [2]. A crucially smaller accessibility of anilines with 3–4 fluorine atoms was significantly alleviated thanks to recent developing the partial reductive hydrodehalogenation of polyfluoroarenes by zinc in aqueous ammonia [3]. Of special importance is the application of this simple reducing system to polyfluorinated *N*-acetanilides [4,5] and chloropolyfluoroanilines [6] to obtain *ortho*-unsubstituted polyfluoroanilines as versatile building blocks for diverse polyfluorobenzo azaheterocycles. Thus, this previously scarcely developed area is really opened up for a systematic intensive elaboration, as exemplified by recent studies of quinolines polyfluorinated on the benzene moiety [5,7].

Fluoronaphthylamines are also of interest for the reasons mentioned above. Thus, practical application have found either monofluoronaphthylamines [8], normally prepared by the traditional methods of fluorine and amino group introduction in an aromatic core, or perfluoro-2-naphthylamine **1** [9,10] and -β-naphthylenediamines accessible outright from octafluoronaphthalene [10]. Unlike this, naphthylamines with 2–6 fluorine atoms in the naphthalene skeleton were almost inaccessible for extensive studies and synthetic application for a long time because the routine methodology for fluorine substitution into an arene core is too tedious in this case. However, the situation promises to somewhat improve thanks to recent extension of the above Zn–aq. NH_3 hydrodefluorination methodology on the *N*-acetyl derivative of amine **1** to afford an unprecedentedly concise route to some polyfluoro-2-naphthylamines containing 1–3 hydrogen atoms in the naphthalene core, in particular *ortho* to the amino group [11]. In these studies the *N*-acetyl derivatives were hydrodefluorinated since polyfluoroanilines were found intact, obviously because of the diminishing their electron affinity (EA) by an electron-donating effect of the amino group [4,5]. However, polyfluoronaphthylamines were expected to have better chance to undergo hydrodefluorination because of the inherently higher EA of the naphthalene core vs. the benzene one. Simultaneously, a quantum chemical study of the mechanism of the *N*-(polyfluoroaryl)acetamides hydrodefluorination, relying on the regioselectivity observed in this reaction, was rather fruitful to elucidate the relationship between the structure of polyfluoroarene radical anions (RAs) as putative short-lived intermediates and the regularities of their fragmentation [5,11].

* Corresponding author. Fax: +7 383 3309752.
E-mail address: shtein@nioch.nsc.ru (V.D. Shteingarts).

0022-1139/$ – see front matter © 2012 Published by Elsevier B.V.
doi:10.1016/j.jfluchem.2012.02.012

Table 1
Conditions and results of the reduction of amine **1**.

No	Substrate (mmol)	Aq. NH_3 (mL, concentration)	Reducer (mmol for Zn or g for the Zn–Cu couple)	Additives	Time (h)	Reaction products[a]	
						Distribution (mol.%[b])	The 7/6 ratio[c]
1	**1** (1.0)	45, 34%	Zn (10.0)		6	**1** (86), **2** (7), **3** (5), **4** (1)	1.6
2	**1** (1.0)	45, 25%	Zn (15.0)		6	**1** (62), **2** (19), **3** (13), **4** (1)	1.5
3	**1** (1.0)	50, 25%	Zn (40.0)		50	**1** (13), **2** (31), **3** (28), **4** (17)	1.7
4	**1** (1.3)	60, 25%	Zn (49.2)	Ethanol (15 mL)	5	**1** (48), **2** (28), **3** (19)	1.5
5	**1** (1.0)	60, 34%	Zn (40.0)	Ethanol (15 mL)	233	**2** (4), **3** (15), **4** (51), **5** (15)	1.8
6	**1** (1.2)	70, 25%	Zn–Cu (4)	Ethanol (10 mL)	22	**4** (56), **5** (16), **6** (11), **7** (10)	2.6
7	**1** (18.6)	690, 25%	Zn–Cu (42)	Ethanol (110 mL)	25	**4** (56), **5** (18), **6** (10), **7** (8)	2.5
8	**3** (0.8)	90, 25%	Zn–Cu (1.8)	Ethanol (8 mL)	21	**3** (17), **5** (49), **7** (9), **10** (20)	
9	**1** (1.0)	45, 25%	Zn (15.0)	NH_4SCN (3.0 mmol)	6	**1** (81), **2** (9), **3** (6)	1.5
10	**1** (1.0)	60, 34%	Zn (40.0)	NH_4SCN (3.0 mmol) Ethanol (5 mL)	233	**2** (13), **3** (26), **4** (44), **5** (6)	2.2
11	**1** (1.2)	70, 25%	Zn–Cu (4)	NH_4SCN (7.0 mmol) Ethanol (10 mL)	22	**3** (9), **4** (46), **5** (15), **6** (4), **7** (2)	1.9

[a] 72–99% total yield.
[b] According to ^{19}F NMR and GC–MS data. When the percentage sum is less than 100%, some minor unidentified components are present.
[c] The correlation of fluorine removals from the 7- and 6-positions.

Hence, purposes of the present work are to examine the feasibility and to reveal the regiochemistry of the reductive hydrodefluorination of amine **1** and its descendant partially defluorinated analogues by Zn and Zn–Cu couple in aqueous ammonia. Cyclic voltammetry (CV) measurements, quantum chemical calculations, and resultant mechanistic consideration are also implemented to further explore the compatibility of the experimentally observed reactivity displayed by polyfluoroarenes upon the reduction by Zn with the mechanism involving formation and fragmentation of a polyfluoroarene RA.

2. Results and discussion

2.1. Reduction of polyfluorinated 2-naphthylamines by zinc in aqueous ammonia

The reduction experiments were carried out analogously to the technique described in Ref. [11]. The conditions and results are presented in Table 1. Keeping in mind the previously observed acceleration of the reaction by adding $ZnCl_2$ [11,12], ethanol, and $CuCl_2$ [5], the effects of these additives in the reaction under study were also checked. The product distributions and structures were inferred from NMR (Table 2) and GC–MS data.

Consistently with the above expectation, upon the action of zinc dust in aqueous ammonia amine **1** gave nearly equal amounts of isomeric once defluorinated 1,3,4,5,6,8- and 1,3,4,5,7,8-hexafluoro-2-naphthylamines **2** and **3** together with doubly defluorinated 1,4,5,6,8-pentafluoro-2-naphthylamine **4** (Table 1, entries 1–3, Scheme 1). Amine **3** was obtained earlier already [11]. Here and below we have not managed to separate the product mixtures and to isolate the individual compounds by TLC. However, the previously unknown amine **2** was unequivocally identified by the GC–MS (see Section 4) and ^{19}F data (vide infra).

The $ZnCl_2$ and NH_4Cl additives, as well as increasing ammonia concentration in the range of 25–34% did not distinctly influence the degree of amine **1** conversion, unlike what was previously found for diverse polyfluoroarenes [12,13]. Assuming the expected accelerating effects to be more or less canceled out by the decreased substrate solubility, an ethanol additive was used in further experiments to somewhat propel the reaction (entries 4 and 5; cf. [13]).

Based on the data for *N*-polyfluoroarylacetamides [5,11], we explored the $CuCl_2$ additive to generate in situ the Zn–Cu couple as a more efficient reducing agent [14] and achieved the distinctly increased conversion of **1** in 25% aqueous ammonia (cf. entries 3 and 6 in Table 1). After 22 h the starting compound and amines **2** and **3** were completely consumed, the double defluorinated amine **4** being a major product. Moreover, the ^{19}F NMR and GC–MS analyses evidenced some amounts of the isomeric doubly defluorinated product – amine **5** and the triply defluorinated amines **6** and **7**. Amines **5** and **7** were obtained previously via hydrodefluorination of *N*-acetyl derivative **11** of amine **1** [11]. To individualize the major product, a re-crystallized fraction consisting of 83% of **4** (entry 7, Table 1) was acetylated to yield *N*-(1,4,5,6,8-pentafluoro-2-naphthyl) acetamide (**8**) (Fig. 1; proved by the X-ray analysis; see Section 4), which was hydrolyzed to the individual amine **4**.

The queues of two fluorines removal leading to amines **4** and **5** are not distinctly clear, but it is reasonably to assume that they are derived, at least significantly, from amines **2** and **3**, respectively. Thus, the **2** to **4** ratio decreased from (13 ± 6):1 at 14–38% conversion to 2:1 at 87% conversion (cf. entries 1–3) and inverted to full conversion of **1** (entry 5). Appearing in the product mixture only after very long reaction time (entry 5), amine **5** arises likely from the consecutive reduction of amine **3**. This assumption is supported by the independent reduction of amine **3** (entry 8). The observed time dependence of the product distribution suggests amine **4** to be formed from amine **2** faster than amine **5** from amine **3**. However, the formation of amine **4** (at least in part) from another product of amine **1** monohydrodefluorination – 1,4,5,6,7,8-hexafluoro-2-naphthylamine **9** (Fig. 1) – cannot be excluded. This implies that amine **9** forms more rapidly than **3** but does not accumulate in the reaction

Table 2
^{19}F and ^{1}H data of polyfluoro-2-naphthylamines ($CDCl_3$).

Compound	Chemical shifts[a] δ (ppm) and spin coupling constants[b] J (Hz)							
	1	2	3	4	5	6	7	8
1	−147.3 (ddd, 1F) $J_{F1,F8}$ = 59 $J_{F1,F4}$ = 16 $J_{F1,F3}$ = 10	4.2 (br.s, 2H, NH_2)	−153.3 (m, 1F)	−150.7 (ddd, 1F) $J_{F4,F5}$ = 57 $J_{F4,F3}$, $J_{F4,F1}$ ≈ 16	−148.3 (ddd, 1F) $J_{F5,F4}$ = 57 $J_{F5,F6}$ = 19 $J_{F5,F8}$ = 16	−161.6 (ddd, 1F) $J_{F6,F5}$ = 19 $J_{F6,F7}$ = 16 $J_{F6,F8}$ = 4	−157.8 (dd, 1F) $J_{F7,F8}$ = 19 $J_{F7,F6}$ = 16	−150.1 (dddd, 1F) $J_{F8,F1}$ = 59 $J_{F8,F7}$ = 19 $J_{F8,F5}$ = 16 $J_{F8,F6}$ = 4
2	−145.9 (ddd, 1F) $J_{F1,F8}$ = 63 $J_{F1,F4}$ = 16 $J_{F1,F3}$ = 11	4.1 (br.s, 2H, NH_2)	−152.2 (m, 1F)	−151.5 (ddd, 1F) $J_{F4,F5}$ = 56 $J_{F4,F1}$ = 16 $J_{F4,F3}$ = 18	−152.6 (dddd, 1F) $J_{F5,F4}$ = 56 $J_{F5,F6}$ = 18 $J_{F5,F8}$ = 16 $J_{F5,H7}$ = 6	−141.4 (m, 1F)	7.0 (ddd, 1H) $J_{H7,F8}$ = 12 $J_{H7,F6}$ = 11 $J_{H7,F5}$ = 6	−120.9 (br.ddd, 1F) $J_{F8,F1}$ = 63 $J_{F8,F5}$ = 16 $J_{F8,H7}$ = 12
3	−148.0 (ddd, 1F) $J_{F1,F8}$ = 57 $J_{F1,F4}$ = 16 $J_{F1,F3}$ = 11	4.3 (br s, 2H, NH_2)	−155.7 (m, 1F)	−150.0 (ddd, 1F) $J_{F4,F5}$ = 63 $J_{F4,F3}$ ≈ 18 $J_{F4,F1}$ = 16	−119.5 (dd, 1F) $J_{F5,F4}$ = 63 $J_{F5,F8}$ = 18	6.9 (ddd, 1H) $J_{H6,F5}$, $J_{H6,F7}$ ≈ 11 $J_{H6,F8}$ = 6	−137.9 (m, 1F)	−154.5 (dddd, 1F) $J_{F8,F1}$ = 57 $J_{F8,F7}$, $J_{F8,F5}$ ≈ 18 $J_{F8,H6}$ = 4
4	−150.2 (ddd, 1F) $J_{F1,F8}$ = 63 $J_{F1,F4}$ = 19 $J_{F1,H3}$ = 6	4.0 (br.s, 2H, NH_2)	6.8 (dd, 1H) $J_{H3,F4}$ = 12 $J_{H3,F1}$ = 6	−122.5 (ddd, 1F) $J_{F4,F5}$ = 61 $J_{F4,F1}$ = 19 $J_{F4,H3}$ = 12	−151.7 (dddd, 1F) $J_{F5,F4}$ = 61 $J_{F5,F6}$, $J_{F5,F8}$ ≈ 18 $J_{F5,H7}$ = 6	−143.3 (ddd, 1F) $J_{F6,F5}$ =18 $J_{F6,H7}$ = 10 $J_{F6,F8}$ = 5	7.0 (ddd, 1H) $J_{H7,F8}$ = 12 $J_{H7,F6}$ = 10 $J_{H7,F5}$ = 6	−121.5 (ddd, 1F) $J_{F8,F1}$ = 63, $J_{F8,F5}$ = 18 $J_{F8,H7}$ = 12
5	−152.3 (ddm, 1F) $J_{F1,F8}$ = 57 $J_{F1,F4}$ = 18	−158.9 (br.s, 1F 2H, NH_2)	6.7 (dd, 1H) $J_{H3,F4}$ ≈ 12 $J_{H3,F1}$ = 6.5	−120.7 (ddd, 1F) $J_{F4,F5}$ = 68 $J_{F4,F1}$ = 18 $J_{F4,H3}$ ≈ 12	−118.3 (ddd, 1F) $J_{F5,F4}$ = 68 $J_{F5,F8}$ ≈ 16 $J_{F5,H6}$ ≈ 12	6.8 (ddd, 1H) $J_{H6,F5}$, $J_{H6,F7}$ ≈ 12 $J_{H6,F8}$ = 6	−137.0 (m, 1F)	−155.0 (dddd, 1F) $J_{F8,F1}$ = 57 $J_{F8,F7}$ ≈ 18 $J_{F8,F5}$ ≈ 16 $J_{F8,H6}$ = 5
6	7.3 (dd, 1H) $J_{H1,F3}$ = 8.5 $J_{H1,H4}$ = 1	3.9 (br.s, 2H, NH_2)	−141.0 (m, 1F)	7.7 (d.d, 1H) $J_{H4,F3}$ ≈ 11 $J_{H1,H4}$ = 1	−153.7 (dm, 1F $J_{F5,F6}$ = 20)	−135.0 (m, 1F)	6.7 (ddd, 1H) $J_{H7,F6}$, $J_{H7,F8}$ ≈ 10 $J_{H7,F5}$ = 6	−127.0 (dm, 1F) $J_{F8,H7}$ = 15
7	7.2 (dd, 1H) $J_{H1,F3}$ = 8.5 $J_{H1,H4}$ = 1	4.3 (br s, 2H, NH_2)	−132.8 (m, 1F)	7.6 (dd, 1H) $J_{H4,F3}$ = 11.5 $J_{H4,H1}$ = 1	−125.6 (m, 1F)	6.8 (ddd, 1H) $J_{H6,F5}$, $J_{H6,F7}$ ≈ 10 $J_{H6,F8}$ = 6	−141.4 (ddd, 1F) $J_{F7,F8}$ = 18 $J_{F7,H6}$ = 10 $J_{F7,F5}$ = 6	−156.8 (dd, 1F) $J_{F8,F7}$, $J_{F8,F5}$ ≈ 18
10	−142.4 (ddm, 1F) $J_{F1,F8}$ = 50 $J_{F1,F3}$ = 14	[c]	−129.7 or −124,3 (m, 1F)	[c]	−124.3 or −129.7 (m, 1F)	[c]	−140.0 (m, 1F)	∼−155.0 (m, 1F)

[a] Standards are cited in Section 4; downfield shifts are positive.
[b] In addition to the cited couplings, many signals contain additional doublet splittings with J = 1–5 Hz due to inter-ring spin couplings (cf. [15d,17]).
[c] Obscured by the overlapping signals.

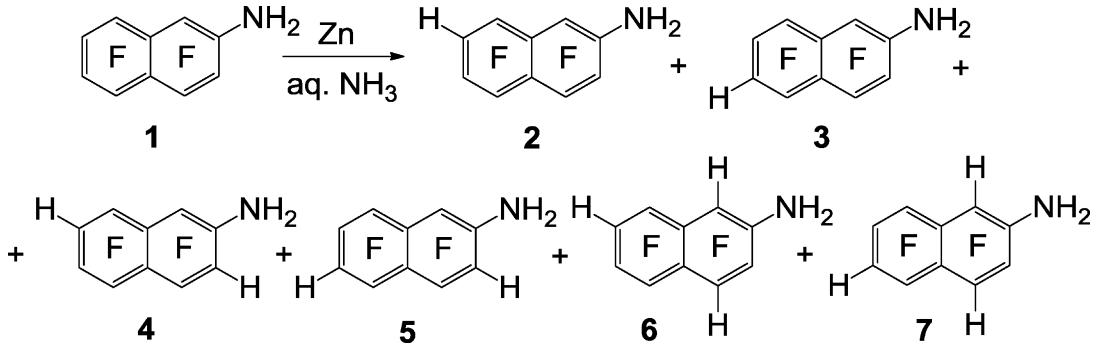

Scheme 1. Hydrodefluorination of amine **1**.

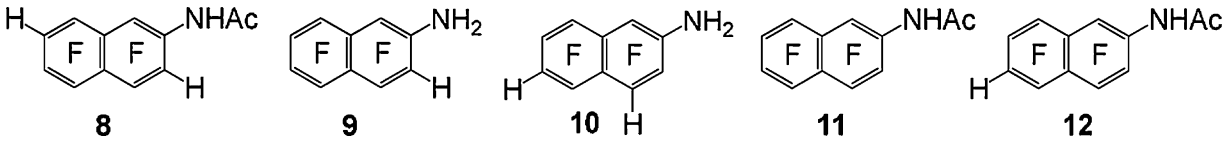

Fig. 1. Structures of compounds **8**–**12**.

mixture due to further easy hydrodefluorination. Importantly, in the product mixture obtained from **3** an appreciable amount (~20%, entry 8) of putative 1,3,5,7,8-pentafluoro-2-naphthylamine **10** (Fig. 1) was present (according to its ^{19}F NMR characteristics, vide infra).

From the above product distributions, amine **1** is inferred to undergo hydrodefluorination less regioselectively compared with its *N*-acetyl derivative **11** (Fig. 1) [11], the correlation of fluorine removals from 7- and 6-positions (the 7/6 ratio) being opposite: the ratio (**2** + **4** + **6**)/(**3** + **5** + **7**) is in the range of (1.5–1.8):1, which slightly increases with reaction time (entries 1–5). Reduction of **1** by the Zn–Cu couple displayed somewhat increased 7/6 ratio (entries 6 and 7), the reliability and possible reason of which are not clear at the moment. The *ortho* hydrodefluorination of *N*-(polyfluoroaryl)acetamides was previously revealed to proceed via a substrate complexation with Zn^{2+}, being either promoted with a Zn salt additive [5] or crucially retarded by ammonium thiocyanate [11]. Unlike this, the latter additive exhibited only a barely discernible (if any) retardation of the amine **1** hydrodefluorination, the products distribution remaining practically the same (cf. entries 2 and 9, 6 and 11). Nevertheless, this does not rule out the possible contribution of the Zn cation complexation because polyfluoroarylamines as ligands can compete more efficiently with a thiocyanate anion for binding with Zn^{2+} compared with their *N*-acetyl derivatives. On the other hand, the polyfluoronaphthylamine hydrodefluorination mainly via the Zn^{2+}-substrate complex can be of doubt because of the lack of appreciable effect of the $ZnCl_2$ additive mentioned above.

2.2. NMR characteristics of polyfluorinated 2-naphthylamines (Table 2)

In order to rationalize the NMR characteristics of previously unknown amines **2**, **4** and **6**, used were amine **1** as a bench mark and the changes in ^{19}F chemical shifts caused by a hydrogen substitution for fluorine in going from octafluoro- to isomeric heptafluoronaphthalenes [15a]. Thus, the signals of fluorines *ortho* to a position of F by H replacement are low-field shifted by 20–30 ppm. If such a replacement occurs in the naphthalene α-position, the signal of *para* fluorine is low-field shifted by ~7 ppm and the signal of *peri* fluorine is high-field shifted by ~10 ppm. The latter is accompanied by disappearance of a doublet splitting with J = 55–70 Hz typical for the interaction of two *peri* fluorine atoms (cf. [15]). The NMR characteristics of amines **3**, **5** and **7** observed in the spectra of product mixtures correspond to those reported earlier for the individual compounds [11]. Overall, the NMR characteristics of polyfluorinated 2-naphthylamines under study are well consistent with the relevant literature data for a wide diversity of polyfluoroarenes [16].

2.3. Reaction mechanism

The mechanistic discussion of the reaction under study is based on the previously substantiated notion (see [5,11] and references therein) that key steps in the reductive hydrodefluorination of polyfluoroarenes are the single electron reduction of a substrate and the subsequent fission of a derived RA to a fluoride anion and a polyfluoroaryl radical. The latter is reduced to a polyfluoroaryl anion, the protonation of which completes the formation of a hydrodefluorination product. With reference to amine **1**, this mechanism is depicted in Scheme 2. Besides, the above possibility should be kept in mind that a substrate is pre-equilibrated with its Zn^{2+}-complex which is believed more electron accepting and, consequently, being reduced more readily compared with a free amine.

2.3.1. Energetics of polyfluoro-2-naphthylamines reduction

The consistency of free amine **1** to undergo hydrodefluorination to produce the products according to Scheme 1 was checked by CV

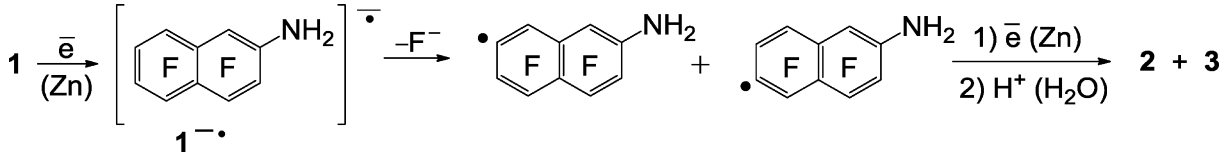

Scheme 2. Mechanism of the amine **1** hydrodefluorination.

Table 3
AEA values of polyfluoroarenes (ROB3LYP/6-31+G*).

Compound	AEA (eV)	
	Gas phase	Water (PCM)
1	0.54	2.22
2	0.39	2.07
3	0.33	2.02
$C_6F_5NH_2$	0.13 [5]	
C_6F_5NHAc	0.74 [5]	2.32 [12]
11	1.06 [12]	2.50

measurements in DMF on a Pt electrode with Et_4NClO_4 (0.1 M) as an electrolyte (ν = 100 mV/s) and SCE as a reference electrode. Three closely located irreversible reduction peaks with $E_p^{1C} = -2.04$ V, $E_p^{2C} = -2.14$ V, and $E_p^{3C} = -2.24$ V were observed. Accordingly, both **3** and **4** exhibited two irreversible peaks with $E_p^{1C} = -2.11$ and -2.14 V, and $E_p^{2C} = -2.23$ and -2.22 V, respectively.

Indicatively, amines **1**–**3** undergo hydrodefluorination by zinc in aqueous ammonia, whereas the more electron accepting *N*-(1,3,4,5,7,8-hexafluoro-2-naphthyl)acetamide **12** (Fig. 1) ($E_p = -1.90$ V) does not without promoting by Zn^{2+} [11]. Consequently, based on the mechanism portrayed in Scheme 2, in the last case the intermediate RA fragmentation is suggested to be rate-limiting rather than the RA generation via substrate reduction. Obviously, one should seek the reason for this in the peculiarities of this RA electronic structure (see below).

The adiabatic EAs (AEAs) of **1**–**3**, calculated by the ROB3LYP/6-31+G* method and presented in Table 3 together with similar data for some compounds essential for the discussion, show that, as predicted (cf. AEA of 0.69 eV for C_6F_6 and 1.02 eV for $C_{10}F_8$ [18]), the naphthylamines possess larger AEAs than $C_6F_5NH_2$, which fails to be reduced under the conditions used in the present work, but smaller than $C_6F_5NHCOCH_3$ and, especially, amide **11**, both being hydrodefluorinated under these conditions without promoting by Zn^{2+} [11].

According to the calculation results, even nonspecific solvation by water increases crucially the AEA values, and this effect is expected to be still more strengthened by the fluorine atoms hydrogen bonding with water molecules (the specific solvation; cf. [19]). Besides, the calculated gas phase AEAs of **1**–**3** fall into a range between C_6F_6 (the experimental values 0.52–0.86 eV, 0.53 eV being most confident [20], the calculated values 0.69–0.72 eV [18,19b,21]) and C_6F_5H (0.32 eV, calculated in this work by the UB3LYP/6-31+G* method), both these polyfluorobenzenes also being hydrodefluorinated by zinc in aqueous ammonia [13]. Thus, the possibility of amines **1**–**3** to be reduced in the used conditions without the Zn^{2+} promotion seems reasonable.

2.3.2. Consideration of the regioselectivity of RA fragmentation based on calculated electronic and spatial structures of polyfluoro-2-naphtylamine RAs

According to Scheme 2, the regioselectivity of reductive defluorination of the amines under study is determined by the regioselectivity of their RAs fragmentation. Keeping in mind the peculiarities of the haloarene RAs fragmentation mechanism [22], one may assume that the more SOMO density is located on a certain C–F bond and, accordingly, this bond is stretched and out-of-plane bent, the more a RA is predisposed to decay on this position [23]. In order to additionally examine the eligibility of such rationalization, the electronic and spatial structures of RAs of the amines were calculated at the ROB3LYP/6-31+G* level. Effects of solvation by water were explored by PCM method. The most probable fragmentation paths for some of these RAs were also calculated and respective transition states (TSs) were located. To clarify the origin of the peculiarities of RA structures, the ROHF/6-31G* calculations of the ground π- and lowest excited σ*-states for the model planar forms of $\mathbf{1}^{-\bullet}$ and $\mathbf{3}^{-\bullet}$ were performed.

The calculated geometries and single occupied MOs (SOMOs) for RAs $\mathbf{1}^{-\bullet}$–$\mathbf{3}^{-\bullet}$ are depicted in Fig. 2. One can see that all the RAs have a non-planar pseudo-π-radical structure. This is due to the vibronic interaction of the RA ground π-state with the low lying excited σ*-state (pseudo-Jahn–Teller effect [24]), the corresponding SOMOs for planar RAs $\mathbf{1}^{-\bullet}$ and $\mathbf{3}^{-\bullet}$ being depicted in Fig. 3. For the gas-phase $\mathbf{1}^{-\bullet}$ the σ*-state admixture to the ground π-state results in the SOMO dispersed over the naphthalene core but unbalanced somewhat in favor of the tetrafluorinated ring (cf. Figs. 2 and 3). So, the gas phase results predict the $\mathbf{1}^{-\bullet}$ fragmentation to occur on the tetrafluorinated ring, but do not prefer any certain C–F bond.

The situation changes dramatically by taking into account nonspecific solvation by water. According to the obtained data (Fig. 2), two energetically close minima appear on the $\mathbf{1}^{-\bullet}$ potential energy surface, each corresponding to the SOMO almost fully located in the tetrafluorinated ring, namely either on the C^7–F or on the C^6–F bond (forms $\mathbf{1a}^{-\bullet}$ and $\mathbf{1b}^{-\bullet}$, respectively; $\mathbf{1a}^{-\bullet}$ is only ~1 kcal/mol thermodynamically preferable compared with $\mathbf{1b}^{-\bullet}$). Such a SOMO location is concomitant with additional significant elongating, out-of-plane deviating and, respectively, preconditioning these C–F bonds to decay. This effect of nonspecific solvation by water was previously calculated for the RA $\mathbf{11}^{-\bullet}$ of amide **11** [11] and is anticipated to be appreciably strengthened by specific solvation [19]. Thus, both water-solvated $\mathbf{1}^{-\bullet}$ and $\mathbf{11}^{-\bullet}$ should be qualified as pseudo-σ-radicals [23].

Unlike $\mathbf{1}^{-\bullet}$, the calculated gas-phase SOMO configurations of $\mathbf{2}^{-\bullet}$ and $\mathbf{3}^{-\bullet}$ exhibit somewhat increased SOMO density in the amino substituted ring at the expense of the other one, and in both cases this disproportion is only little enhanced by the solvation. Thus, in comparison with $\mathbf{1}^{-\bullet}$, this supports the conclusion made earlier for $\mathbf{11}^{-\bullet}$ [11] that the predominant concentration of a negative charge in the tetrafluorinated ring is a combined effect of solvation by the highly polar solvent and one-by-one location of the four fluorine atoms. These SOMO configurations are concomitant with distinctly larger stretching and out-of-plane deviation of bonds C^3–F in $\mathbf{2}^{-\bullet}$ or C^3–F and C^4–F in $\mathbf{3}^{-\bullet}$ compared with other C–F bonds.

Concerning reality of the above effect of four nearby fluorine atoms, the break of this structural unit should appreciably diminish the electron-accepting capacity of the ring not only due to the removal of one fluorine atom, but also because of destroying their one-by-one location. This is justified by the UB3LYP/6-31+G* calculated AEA values of 1,2,3,4-tetrafluorobenzene (−0.05 eV), 1,2,3,5-tetrafluorobenzene (−0.11 eV), and 1,2,4,5-tetrafluorobenzene (−0.23 eV). Moreover, whereas the π-SOMO of the planar $\mathbf{1}^{-\bullet}$ is practically evenly dispersed over two rings, its σ*-SOMO is completely located in the tetrafluorinated ring (Fig. 3), that manifests itself in the SOMO configuration of the water-solvated $\mathbf{1}^{-\bullet}$ (Fig. 2). This clearly reveals the nearby fluorines effect to be of σ-electronic nature, thus obviously lowering the σ*-state in energy, strongly elongating and bending out the C–F bonds of the tetrafluoro-substituted ring. Unlike this, the SOMO of $\mathbf{3}^{-\bullet}$ (Fig. 2) insignificantly differs from the π-SOMO of the planar $\mathbf{3}^{-\bullet}$, the latter looking like a blend of π-states of the planar $\mathbf{1}^{-\bullet}$ and 2-H-heptafluoronaphthalene RA ($2\text{-}HC_{10}F_7^{-\bullet}$, Fig. 3). Indicatively, the σ*-SOMO of $2\text{-}HC_{10}F_7^{-\bullet}$ is also almost completely located in the tetrafluorinated ring.

Having analyzed the above computational results, one may compare them with the experimental hydrodefluorination regioselectivity of amines **1**–**3**. With this purpose, the geometry parameters of selected C–F bonds in the RAs and, in some cases, in the respective fragmentation TSs are related to the corresponding energy barriers in

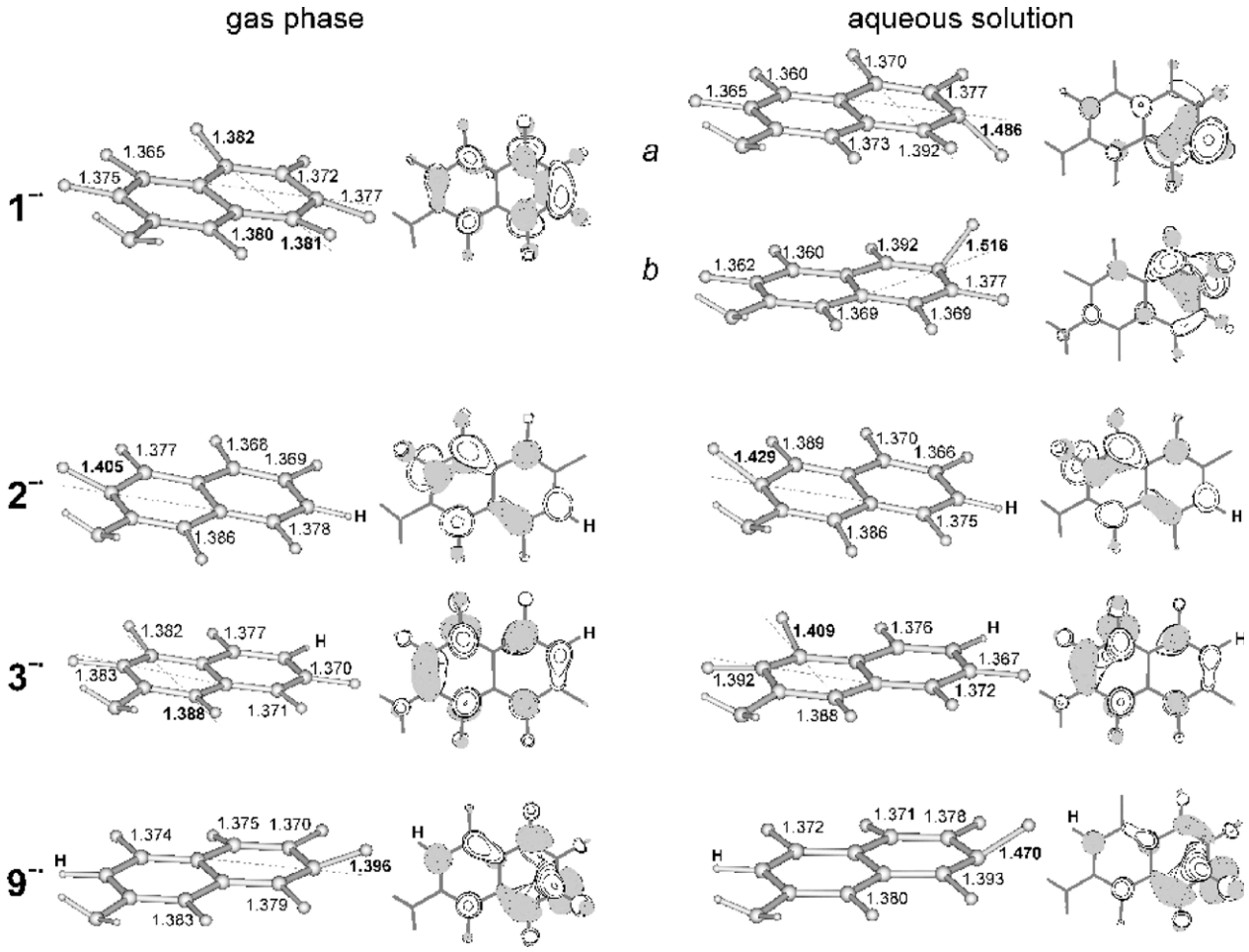

Fig. 2. Spatial structures and SOMOs of polyfluoro-2-naphthylamine RAs (the bond length are given in Å).

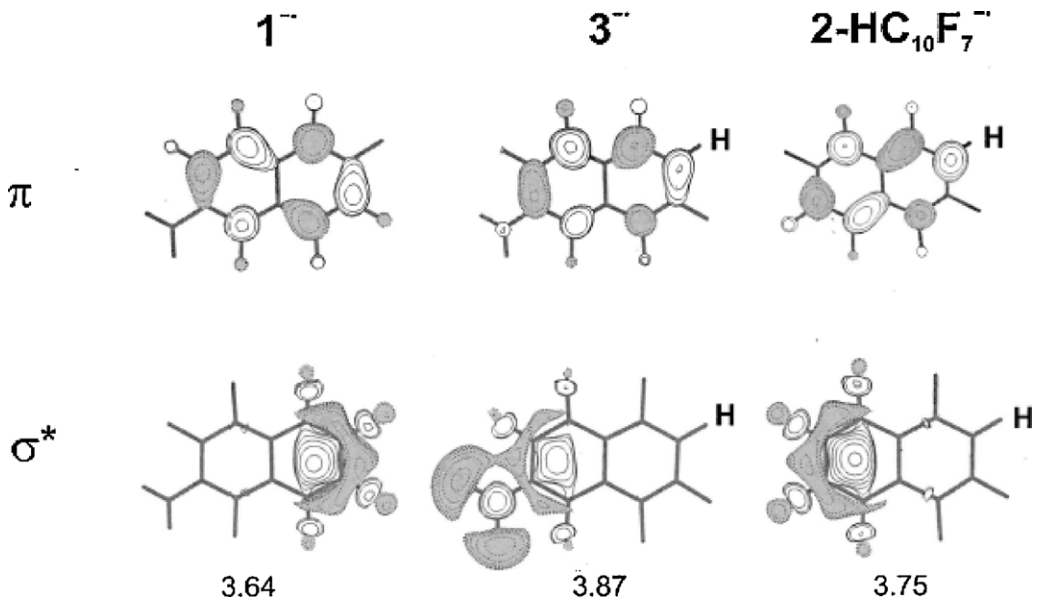

Fig. 3. SOMOs of ground π- and excited σ*-state for planar $\mathbf{1}^{-\bullet}$, $\mathbf{3}^{-\bullet}$, and 2-$HC_{10}F_7^{-\bullet}$ (the σ*-energies are given in eV relative to the π-energy = 0).

Table 4. One can see that C–F bond lengths and out-of-plane deviations change concertedly, both obviously characterizing (other things being equal) the predisposition of a C–F bond to decay and, consequently, correlating qualitatively with the respective positional energy barriers. An easy C-7-hydrodefluorination of the amine **9** as possibly first formed from amine **1** also seems quite real because the presence of the tetrafluorinated benzene moiety should provide this compound with a sufficient EA and its RA $\mathbf{9}^{-\bullet}$ with an appropriate electronic and spatial structures (Fig. 2, Table 4), the C^7–F bond being most predisposed to cleave.

Table 4
Geometry parameters of selected C–F bonds in RAs or TSs of their cleavage with the F^- expulsion, and the respective energy barriers (ROB3LYP/6-31+G*).

RA-position	RA		TS		Increase in going from RA to TS		Energy barrier for the F^- expulsion (kcal/mol)
	Length (Å)	Deviation (°)	Length (Å)	Deviation (°)	Length (Å)	Deviation (°)	
1b$^{-\bullet}$-6	1.516	40.3	1.603	43.4	0.087	3.1	0.1
1a$^{-\bullet}$-7	1.486	38.4	1.655	43.3	0.169	4.9	0.4
1a$^{-\bullet}$-3	1.365	0.0	1.652	41.2	0.287	41.2	4.7
2$^{-\bullet}$-3	1.429	26.2					
3$^{-\bullet}$-3	1.392	8.8	1.605	41.3	0.213	32.5	1.3
3$^{-\bullet}$-4	1.409	21.9	1.685	47.4	0.276	25.5	1.5
9$^{-\bullet}$-7	1.470	35.9					

Following the above reasons and the computational results (Fig. 2, Table 4), RA **1**$^{-\bullet}$ is predicted to undergo practically barrierless fragmentations on the C^7–F and C^6–F bonds. Indicatively in this respect, these bonds are enormously stretched and out-of-plane bent, thus approaching their counterparts in the corresponding TSs. These structural peculiarities of **1**$^{-\bullet}$ agree nicely with the formation of amines **2** and **3** upon the amine **1** hydrodefluorination, amine **2** forming somewhat predominantly, obviously, due to the slight prevalence of **1a**$^{-\bullet}$ above **1b**$^{-\bullet}$ (vide supra). At the same time, the **1**$^{-\bullet}$ fragmentations on the other C–F bonds are clearly predicted less probable. Particularly, the energy barrier for the C^3–F bond cleavage was calculated more than 4 kcal/mol higher compared with that for the C^7–F bond (Table 4).

The predicted (Fig. 2 and Table 4) decays on the C^3–F bond for **2**$^{-\bullet}$ and on the C^3–F and C^4–F bonds for **3**$^{-\bullet}$ are fully in line with the predominant formation of amine **4** from **2** and amines **5** and (putative) **10** from **3**, respectively. However, in the latter case the distribution of the monohydrodefluorination products agrees with the calculated bond elongations in going from the RA to the TSs and with the respective energy barriers, rather than with the bond bendings, the latter for the C^3–F bond looking anomalously small.

The above fact that amines **2** and **3** are defluorinated under the used conditions despite their smaller EA values compared with amide **12** (the latter remaining intact without Zn^{2+} promotion [11]) can be an evidence for the RA fragmentation rather than formation to be the rate-limiting stage in hydrodefluorination of amide **12**. To reveal how this may result from some unusual peculiarities of **12**$^{-\bullet}$, one should compare its SOMO configuration and spatial structure calculated before [11] with those of **3**$^{-\bullet}$. Indeed, unlike **3**$^{-\bullet}$, **12**$^{-\bullet}$ presents a quite rare example of a planar polyfluoroarene RA with the practically undisturbed π-type SOMO, thus being symmetry forbidden for easy fragmentation [23].

As mentioned above, for the alternative reaction course leading to amines **4** and (less probably) **5** considered should be the primary hydrodefluorination of **1** at the 3-position followed by the very fast hydrodefluorination of amine **9** thus formed. According to the above energy barrier arguments, the 3-position hardly can compete with the 6- and 7-positions to be a principal site for hydrodefluorination of amine **1**. Additionally, the calculated spatial structure and SOMO configuration of **9**$^{-\bullet}$ exhibit no substantial difference between the gas phase and aqueous solution states, both clearly favoring the decay on the C^7–F bond but not on the C^6–F bond. This means that **4** but not **5** could obviously be formed via **9**.

2.3.3. Probing the anionic σ-complex approximation

The anionic σ-complex approximation to modeling TSs of haloarene RA fragmentation [25] is a simple tool for the routine qualitative rationalization and prediction of outcomes of these synthetically important reactions with using well-known regioselectivity regularities of polyfluoroarene reactions with nucleophiles [10,26]. It was previously shown to work for hydrodefluorination of a wide series of polyfluoroarene derivatives [3–5,11–13], including 2-acetamidoheptafluoronaphthalene [11]. However, there were no such data for polyfluoroarylamines. To explore the applicability of this approximation to the polyfluoro-2-naphtylamines hydrodefluorination, we performed PBE/3z calculations of the σ-complexes corresponding to a fluoride anion addition to all positions of amines **1**–**3** occupied by fluorine atoms. The calculated relative energies of these complexes are presented in Table 5.

These data reveal that the relative stabilities of σ-complexes corresponding to the fluoride anion addition at the tetrafluorinated ring reproduces qualitatively the regioselectivity of the amine **1** hydrodefluorination and, respectively, the **1**$^{-\bullet}$ fragmentation of lowest energy is the σ-complex of the F^- addition to C^7 (the C^7 σ-complex) and the next in the energy scale is the C^6 σ-complex. However, this coincidence is evidently not meaningful in terms of the original rationale of σ-complex approximation [25] because **1**$^{-\bullet}$ is a strongly pronounced pseudo-σ-RA decaying almost barrierlessly, so that its fragmentation regioselectivity is obviously determined by the **1a**$^{-\bullet}$/**1b**$^{-\bullet}$ ratio (vide supra) rather than by the ratio of the respective activation barriers.

Of special attention is a disparity between the low relative energy of the C^3 σ-complex (Table 5) and the lack of a clear experimental evidence for the C^3 hydrodefluorination of amine **1**. The structure of RA **1**$^{-\bullet}$ (Fig. 2) displays no prerequisites for the C^3–F fragmentation: the SOMO density should be transferred from the tetrafluorinated ring to the amino substituted one; the strongly stretched and out-of-plane distorted C^7–F or C^6–F bond should shorten and come to the core plane, the opposite occurring with the C^3–F bond. Taking into account these energy consuming transformations is far beyond a competence of the σ-complex approximation.

Unlike this, the large out-of-plane bending (Fig. 2) and, as a consequence, the cleavage of the C^3–F bond in **2**$^{-\bullet}$ and **3**$^{-\bullet}$ as well as of the C^4–F bond in **3**$^{-\bullet}$ agree nicely with the σ-complex predictions (Table 5). However, the C^5–F fragmentation of **3**$^{-\bullet}$ is predicted to occur more readily compared with its C^4–F fragmentation (Table 5) but has no confirmation in the above product distribution. This is in compliance with the calculated structure of **3**$^{-\bullet}$ (Fig. 2). The reasons of the σ-complex approach invalidity in this case are obviously analogous to those considered above for the collision of C^6–F and C^3–F fragmentations of **1**$^{-\bullet}$.

Summing up, the anionic σ-complex approximation is only restrictedly applicable to rationalize the fragmentation regioselectivity of polyfluoronaphthalene (and, obviously, polynuclear

Table 5
Relative energies (kcal/mol) of σ-complexes of amines **1**–**3** with F^- (PBE/3z).

Amine	Position						
	1	3	4	5	6	7	8
1	3.85	0.17	2.23	1.50	1.09	0	2.24
2	3.71	0	4.14	5.18	3.39		2.73
3	3.85	0	0.29	0.18		0.62	4.05

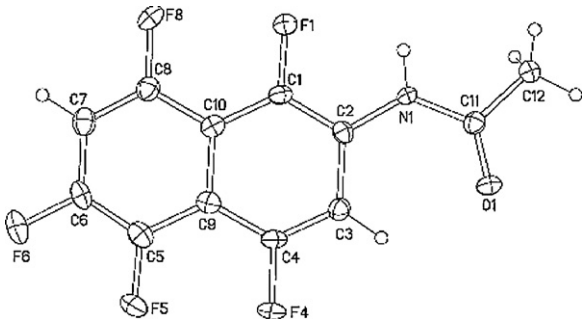

Fig. 4. Spatial structure of amide **8** according to the X-ray data.

polyfluoroarenes in general) RAs which issues from its inherent weakness as a roughly qualitative approach, not taking into account the degree of the RA pseudo-σ-character and out-of-plane distortion. One may suggest the approximation to rather satisfactorily predict a competition of the C–F bonds located in the same ring of a substantially pseudo-π-type RA, the other ring being close to planarity. However, inasmuch as the latter may not be held for the C–F bonds located in different rings, the applicability of this approach to their competition is problematic. On the whole, the polyfluoroarene RA fragmentation is elucidated once more as a reaction not obeying the linear free energy relationship (cf. [27]).

3. Conclusion

Unlike previously studied polyfluoroanilines, heptafluoro-2-naphthylamine has been shown to undergo hydrodefluorination by zinc in aqueous ammonia to give sequentially the products of mono (7- and 6-H-hexafluoro-2-naphthylamines **2** and **3**), di (3,7- and 3,6-H_2-pentafluoro-2-naphthylamines **4** and **5**) and more deeply defluorinated 2-naphthylamines that is due to inherently higher electron affinity of the naphthalene core compared with the benzene one. The reaction regioselectivity agrees nicely with the predicted one based on ab initio calculated electronic and spacial structures of the putative key intermediates – the naphthylamine RAs as a crucial reason determining the regioselectivity of their fragmentation. The calculations reveal the dramatic combined effect of the nonspecific solvation and four nearby fluorine atoms causing the amine **1** water-solvated RA to be a pronounced *pseudo*-σ-radical with an extra electron density almost completely located on the C^6–F or C^7–F bond. This is concomitant with the enormous stretching and out-of-plane deviation of these C–F bonds and, as a consequence, with their practically barrierless decay. Unlike this, the gas phase RA of amine **1** possess the *pseudo*-π-character with an extra electron density nearly evenly dispersed over both ring moieties. According to the calculation results, the break of the four nearby fluorine arrangement by removing F^6 or F^7 completely eliminates this water solvation effect, so that the RAs of amines **2** and **3** are of the *pseudo*-π-character both in a gas phase and in a water solution. The anionic σ-complex approximation has been shown only restrictedly applicable to rationalize the fragmentation regioselectivity of polyfluoroarene RA owing to not taking into account a degree of the RA *pseudo*-σ-character and out-of-plane distortion.

4. Experimental

4.1. General

^{19}F and ^{1}H NMR spectra were recorded on a Bruker AV-300 and a Bruker AM-400 spectrometers, internal standards – C_6F_6 ($\delta_F = -163.0$ ppm) and residual protons in deuterated solvents, respectively. *HRMS data* were obtained with a "DFS" spectrometer.

The GC–MS analyses were performed with a Hewlett–Packard G1081A apparatus, consisting of a gas chromatograph HP 5890 series II and a mass-selective detector HP 5971 (electron impact, 70 eV) by using a 30 mm × 0.25 mm × 0.25 mm column with HP-5 oil.

The CV measurements on degassed $2{\cdot}10^{-3}$ M solutions of compounds **1**, **3**, and **4** in DMF were performed at 295 K in an argon atmosphere using SVA-1BM potentiostat equipped with a Lab-Master analog-to-digital converter with multifunctional interface (Institute of Nuclear Physics, Russian Academy of Sciences, Novosibirsk). The measurements were carried out in three-electrode electrochemical cell ($V = 5$ mL) at a stationary platinum electrode ($S = 8$ mm^2) with 0.1 M Et_4NClO_4 as supporting electrolyte. The sweep rate was 100 mV/s, the peak potentials were quoted with reference to a saturated calomel electrode.

XRD data were obtained on a Bruker Kappa Apex II CCD diffractometer using φ, ω scans of narrow (0.5°) frames with Mo Kα radiation ($\lambda = 0.71073$ Å) and a graphite monochromator. The structures were solved by direct methods and refined by full-matrix least-squares method against all F^2 in anisotropic approximation using the *SHELX-97* programs set [28]. The H atoms positions were calculated with the riding model. Absorption corrections were applied empirically using *SADABS* programs. Compound **8** is monoclinic, space group $P2_1$, $a = 6.0680(8)$, $b = 9.501(1)$, $c = 9.484(1)$ Å, $\beta = 107.977(6)°$, $V = 520.1(1)$ Å^3, $Z = 2$, $C_{12}H_6F_5NO$, $D_c = 1.757$ g/mL, $\mu = 0.174$ mm^{-1}, $F(0\,0\,0) = 276$, crystal size 0.20 mm × 0.10 mm × 0.02 mm, independent reflections 1869, w$R_2 = 0.1132$, $S = 1.06$ for all reflections ($R = 0.0408$ for 1722 $F > 4\sigma$). The obtained crystal structures were analyzed for short contacts between non-bonded atoms using the *PLATON* program [29]. Tables listing detailed crystallographic data, atomic positional parameters, and bond lengths and angles are available as CCDC 761337 from the Cambridge Crystallographic Data Centre via http://www.ccdc.cam.ac.uk/data_request/cif.

The molecular structure of amide **8** is illustrated in Fig. 4. The bond lengths and bond angles are the same as the statistical means [30]. According to the X-ray diffraction data molecules of **8** are perfectly planar in the crystal. The standard deviations from the mean plane are 0.041 Å. The short distances N^1–H···O^1 (2.17 Å) and C^{12}–H···F^1 (2.19 Å) lead to the formation of 2D networks. Note, that normal H···O and H···F contacts are 2.68 Å and 2.56 Å [31]. Additionally to the H···O and H···F interactions, the C–F···π interaction of the fluorine atom of the C^6–F^6 bond of one molecule with the fluorinated hydrocarbon ring of another is observed, the atom-to-plane distance is 3.26 Å.

Quantum-chemical calculations. The geometry of stationary structures (minima and transition states) of RAs was optimized at the ROB3LYP/6-31+G* level of calculations. The same level of theory was used for calculations of their respective neutral molecules. The types of stationary points on RA's potential energy surfaces were determined by normal vibration analysis. Relations between the transition states and minima were established by intrinsic reaction coordinate (IRC) calculations. AEA values were calculated by the UB3LYP method. Effects of solvation were realized by PCM method. These calculations were performed with the program package GAMESS [32]. The structure images and SOMO plots were made by the MOLDEN program [33]. The DFT calculations of anionic σ-complex were performed by the PRIRODA program package [34] using pure PBE functional [35] and the original 3z basis set (that is of TZ2P-quality) integrated to the package. In this program the expansion of molecular electronic density in atom-centered auxiliary basis sets is used for the evaluation of Coulomb and exchange-correlation terms. Such an approach was shown [34] to be about one order of magnitude

faster than usual approaches in which only Coulomb terms are treated using the approximated density.

Materials. Compound **1** was prepared according to the literature procedure [10]. Aqueous ammonia (25%) was "Pure" grade and additionally saturated with gaseous ammonia to obtain a 34% (d = 0.88 g/mL) solution. Activated zinc (powder) was prepared by the literature protocol [5], Zn–Cu couple – by the protocol [7c]. Solvents and reagents were of commercial reagent quality.

4.2. Hydrodefluorination procedures

4.2.1. General procedure

A mixture of the substrate, ammonia solution, Zn powder or Zn–Cu couple and, when used, an additive was stirred at ambient temperature for the specified time (Table 1). Then the mixture was allowed to settle, filtered, organic products were extracted by CH_2Cl_2 both from the filtrate and the precipitate. Combined extracts were dried with $MgSO_4$ and the solvent was evaporated. The residue was analyzed by GC–MS and by NMR. The results are presented in Tables 1 and 2. For previously unknown amines **2**, **6**, and **10** the relevant molecular masses 251, 215, and 233, respectively, were fixed by GC–MS. For formerly described amines **3**, **5**, and **7** their respective molecular masses were also fixed and the ^{19}F NMR signals corresponding to the reported ones [11] were observed.

4.2.2. N-(1,4,5,6,8-pentafluoro-2-naphthyl)acetamide (8)

The product mixture (3.62 g) obtained from the reaction of amine **1** with Zn–Cu couple (entry 7 in Table 1) was crystallized from hexane to give two fractions containing 52% of **4** and 27% of **5** (1.2 g) or 83% of **4** and 9% of **5** (1.06 g), respectively. The latter mixture was treated with Ac_2O (0.94 g) in benzene (35 mL) analogously to the reported protocol [12]. The product was crystallized from ethanol and trice from $CHCl_3$ to yield amide **8** (0.52 g); mp 188–190 °C. Anal. Calcd. for $C_{12}H_6F_5NO$: C, 52.36; H, 2.18; F, 34.55; N, 5.09. Found: C, 51.96; H, 2.17; F, 34.61; N, 5.05.

4.2.3. 1,4,5,6,8-Pentafluoro-2-naphthylamine (4)

A mixture of amide **8** (0.14 g), conc. HCl (10 mL), and ethanol (2 mL) was refluxed for 30 min, cooled, diluted with water (20 mL), and weakly alkalified by conc. aqueous NaOH. The mixture was extracted with CH_2Cl_2 (3× 20 mL), the extract was dried with $MgSO_4$, the solvent was evaporated to yield amine **4** (0.12 g, 97%); mp 178–180 °C. Anal. Calcd. for $C_{10}H_4F_5N$: F, 40.77; N, 6.00. Found: F, 40.78; N, 5.92.

Acknowledgement

The authors are grateful to the Russian Foundation of Basic Research for the financial support (grants 09-03-00248 and 08-03-00495).

References

[1] R. Filler, Y. Kobayashi, L.M. Yagupolskii (Eds.), Organofluorine Compounds in Medicinal Chemistry and Biomedical Applications, Elsevier, Amsterdam, 1993;
R.E. Banks, B.E. Smart, J.C. Tatlow (Eds.), Organofluorine Chemistry. Principles and Commercial Applications, Plenum Press, New York, 1994;
K.L. Kirk, J. Fluorine Chem. 127 (2006) 1013–1029;
C. Isanbor, D. O'Hagan, J. Fluorine Chem. 127 (2006) 303–319;
I. Ojima (Ed.), Fluorine in Medicinal Chemistry and Chemical Biology, Wiley-Blackwell, Chippenham, 2009.
[2] (a) R.E. Florin, W.J. Pummer, L.A. Wall, J. Res. Natl. Bur. Stand. 62 (1959) 107–112;
(b) L.G. Belf, M.W. Buxton, J.F. Tilney-Bassett, Tetrahedron 23 (1967) 4719–4727;
(c) T.D. Petrova, V.P. Mamaev, G.G. Yakobson, Izv. Akad. Nauk SSSR, Ser. Khim. (1969) 679–682.
[3] V.D. Shteingarts, J. Fluorine Chem. 128 (2007) 797–805.
[4] S.S. Laev, V.U. Evtefeev, V.D. Shteingarts, J. Fluorine Chem. 110 (2001) 43–46.
[5] S.S. Laev, Y.L. Gurskaya, G.A. Selivanova, I.V. Beregovaya, L.N. Shchegoleva, N.V. Vasil'eva, M.M. Shakirov, V.D. Shteingarts, Eur. J. Org. Chem. (2007) 306–316.
[6] G.A. Selivanova, Y.L. Gurskaya, L.M. Pokrovsky, V.F. Kollegov, V.D. Shteingarts, J. Fluorine Chem. 125 (2004) 1829–1834.
[7] (a) E.V. Panteleeva, V.D. Shteingarts, J. Grobe, B. Krebs, M.U. Triller, H.Z. Rabeneck, Anorg. Allg. Chem. 629 (2003) 71–82;
(b) Y.L. Safina, G.A. Selivanova, Y.I. Bagrjanskaja, V.D. Shteingarts, Russ. Chem. Bull. Int. Ed. (2009) 1022–1033;
(c) Y.L. Safina, G.A. Selivanova, Y.K. Koltunov, V.D. Shteingarts, Tetrahedron Lett. 50 (2009) 5245–5247.
[8] (a) M.E. Salvati, J.A. Balog, D.A. Pickering, S. Giese, A. Fura, W. Li, R.N. Patel, R.L. Hanson. WO 2002024702, C.A. 136:279441;
(b) M.E. Salvati, T. Mitt, R.N. Patel, R.L. Hanson, D. Brzozowski, A. Goswami, L.N.H. Chu, W.-S. Li, J.H. Simpson, M.J. Totleben, W. He, US 20050119228, C.A. 143:26585r;
(c) H.R. Howard, US 20020004504, C.A. 136:85832x;
(d) S.J. Romano, US 2004100954, C.A. 141:420460g;
(e) S.M. Goldin, S. Katragadda, L.Y. Hu, N.L. Reddy, J.B. Fischer, A.G. Knapp, L.D. Margolin, US 1995, 5403861 A, C.A. 123:132884j;
(f) B. Zhu, Z.J. Jia, W. Huang, Y. Song, J. Kanter, R.M. Scarborough, US 20020091116, C.A. 137:93747j.
[9] (a) B. Gething, C.R. Patrick, J.C. Tatlow, J. Chem. Soc. (1962) 186–190;
(b) F.I. Abezgauz, S.V. Sokolov, S.N. Ezerskij, Zh. Vses. Khim. Obshchestva im. D.I. Mendeleeva 10 (1965) 113–114, C.A. 62:16152h;
(c) D. Price, H. Suschitzky, J.I.J. Hollies, J. Chem. Soc. C (1969) 1967–1973.
[10] T.A. Vaganova, S.Z. Kusov, V.I. Rodionov, I.K. Shundrina, G.E. Sal'nikov, V.I. Mamatyuk, E.V. Malykhin, J. Fluorine Chem. 129 (2008) 253–260.
[11] A.V. Reshetov, G.A. Selivanova, L.V. Politanskaya, I.V. Beregovaya, L.N. Shchegoleva, N.V.I. Vasil'eva, Y. Bagryanskaya, V.D. Shteingarts, ARKIVOC (viii) (2011) 242–262.
[12] S.S. Laev, V.D. Shteingarts, J. Fluorine Chem. 96 (1999) 175–185.
[13] S.S. Laev, V.D. Shteingarts, J. Fluorine Chem. 91 (1998) 21–23.
[14] (a) Zn/Cu couple means that zinc particles are coated with metallic copper formed by reduction of the added copper salt. This is one of the routine methods to *in situ* generate the Zn/Cu couple.
(b) L.F. Fieser, M. Fieser, Reagents for Organic Synthesis, John Wiley and Sons, New York, London, Sydney, 1968, p. 1292.
[15] (a) L.S. Kobrina, V.D. Shteingarts, L.N. Shchegoleva, Izv. Sib. Otd. Akad. Nauk SSSR, Ser. Khim. Nauk (1) (1974) 68–77, C.A. 80: 126541;
(b) F.B. Mallory, J. Am. Chem. Soc. 95 (1973) 7747–7752;
(c) F.B. Mallory, C.W. Mallory, W.M. Ricker, J. Am. Chem. Soc. 96 (1974) 4770–4771;
(d) R.S. Matthews, Org. Magn. Reson. 18 (1982) 226–229.
[16] (a) R.J. Abraham, D.B. Macdonald, E.S. Pepper, J. Am. Chem. Soc. 90 (1968) 147–153;
(b) M.G. Hogben, W.A.G. Graham, J. Am. Chem. Soc. 91 (1969) 283–286;
(c) R.J. Abraham, D.B. Macdonald, E.S. Pepper, J. Chem. Soc. (1967) 835–841;
(d) M.J. Fifolt, S.A. Sojka, R.A. Wolfe, D.S. Hojnicki, J. Org. Chem. 54 (1989) 3019–3023;
(e) L.N. Pushkina, A.P. Stepanov, V.S. Zhukov, A.D. Naumov, Zh. Org. Khim. 8 (1972) 586–597.
[17] R.S. Matthews, J. Magn. Reson. 29 (1978) 65–78.
[18] Y. Xie, H.F. Schaefer III, F.A. Cotton, Chem. Commun. (2003) 102–103.
[19] (a) H. Schneider, K.M. Vogelhuber, J.M. Weber, J. Chem. Phys. 127 (2007) 114312;
(b) S.N. Eustis, Di Wang, K.H. Bowen, G.N. Patwari, J. Chem. Phys. 127 (2007) 114312.
[20] J. Langer, I. Dabkowska, Y. Zhang, E. Illenberger, Phys. Chem. Chem. Phys. 10 (2008) 1523–1531, and references therein.
[21] X.-J. Hou, M.B. Huang, J. Mol. Struct. (Theochem.) 638 (2003) 209–214.
[22] I.V. Beregovaya, L.N. Shchegoleva, Chem. Phys. Lett. 348 (2001) 501–506.
[23] P.V. Schastnev, L.N. Shchegoleva, Molecular Distortions in Ionic and Excited States, CRC Press, Boca Raton, 1995.
[24] I.B. Bersuker, The Jahn–Teller effect, Cambridge University Press, Cambridge, 2006.
[25] P.K. Freeman, R. Srinivasa, J. Org. Chem. 52 (1987) 252–256.
[26] (a) J. Burdon, Tetrahedron 21 (1965) 3373–3380;
(b) J. Burdon, W.B. Hollyhead, J. Chem. Soc. (1965) 6326–6328;
(c) R.D. Chambers, M.J. Seabury, D.L.H. Williams, N. Hughes, J. Chem. Soc., Perkin Trans. 1 (1988) 251–254;
(d) G.W. Dillow, P. Kebarle, J. Am. Chem. Soc. 110 (1988) 4877–4882;
(e) R.D. Chambers, P.A. Martin, G. Sandford, D.L.H. Williams, J. Fluorine Chem. 129 (2008) 998–1002, and references therein.
[27] V.V. Konovalov, S.S. Laev, I.V. Beregovaya, L.N. Shchegoleva, V.D. Shteingarts, Y.D. Tsvetkov, I.I. Bilkis, J. Phys. Chem. A 104 (2000) 352–361.
[28] G.M. Sheldrick, SHELX-97 – Programs for Crystal Structure Analysis (Release 97-2), University of Goetingen, Goettingen, Germany, 1970.
[29] A.L. Spek, PLATON, a Multipurpose Crystallographic Tool (Version 10M), Utrecht University, Utrecht, The Netherlands, 2003.
[30] F.H. Allen, O. Kenard, D.G. Watson, L. Bramer, A.G. Orpen, R. Taylor, J. Chem. Soc., Perkin Trans. 2 (1987) S1–S19.
[31] R.S. Rowland, R. Taylor, J. Phys. Chem. B 100 (1996) 7384–7391.
[32] M.W. Schmidt, K.K. Baldridge, J.A. Boatz, S.T. Elbert, M.S. Gordon, J.H. Jensen, S. Koseki, N. Matsunaga, K.A. Nguyen, S.J. Su, T.L. Windus, M. Dupuis, J.A. Montgomery, J. Comput. Chem. 14 (1993) 1347–1363.
[33] G. Schaftenaar, J.H. Noordik, J. Comput. Aided Mol. Des. 14 (2000) 123–134.
[34] (a) D.N. Laikov, Chem. Phys. Lett. 281 (1997) 151–156;
(b) D.N. Laikov, Y.A. Ustynyuk, Russ. Chem. Bull. Int. Ed. 54 (2005) 820–826.
[35] J.P. Perdew, K. Burke, M. Ernzerhof, Phys. Rev. Lett. 77 (1996) 3865–3868.